Towards Very-Low Latency Storm Nowcasting through AI-Based On-Board Satellite Data Processing

Robert Hinz[1], Álvaro Morón[1], Juan Ignacio Bravo[1], Murray Kerr[1], Cecilia Marcos[2], Antonio Latorre[1] and Francisco Membibre[1]

[1]DEIMOS Space S.L.U., 28760, Tres Cantos – Madrid, Spain
[2]Agencia Estatal de Meteorología, Spain

Abstract

Satellite-based Earth Observation (EO) is a key technology for applications like emergency management, civilian security, and environment and resource monitoring. Demands on amount, type and quality of remote-sensing satellite data and efficient methods for data analysis have increased sharply in recent years. However, the use of satellite-based image products for scenarios which require very low-latencies, such as rapid meteorological and civil security applications, is still limited by the bottleneck created by the classical EO data chain, which involves the acquisition, compression, and storage of sensor data onboard the satellite, and its transfer to ground for further processing. Onboard processing offers a promising solution to reduce the latencies between data acquisition and product delivery to the end user. The H2020 EU project EO-ALERT (http://eo-alert-h2020.eu) implements this approach through the development of a next-generation EO data processing chain that moves optimised key elements from the ground segment to onboard the satellite. In this article, the feasibility of the concept is demonstrated using EO-ALERT's extreme weather nowcasting product as an example. The system is able to detect and track convective storms and Overshooting Tops, and to send the processed information to ground, within 5 minutes of the observation.

Keywords

Earth Observation, On-Board Processing, AI, Low latency, Nowcasting, Satellite Architecture

1. Introduction

In many EO scenarios including environment and resource monitoring, emergency management and civilian security, EO products are only useful if available in a very short time period. However, the use of satellite EO-based image products for rapid meteorological and civil security applications is still limited by the bottleneck created by the classical EO data chain, which involves the acquisition, compression, and storage of sensor data onboard the satellite, and its transfer to ground for further processing. This introduces long latencies until product delivery to the end user.

The H2020 EU project EO-ALERT [1, 2] (http://eo-alert-h2020.eu) a collaboration of several partner organizations (DEIMOS Space (Leader), DLR, OHB Italy, Politecnico di Torino, TU-GRAZ), addresses this problem through the development of a next-generation EO data processing chain that moves optimised key elements from the ground segment to onboard the satellite. Applying optimised Machine Learning (ML) methods, EO products are generated directly onboard the spacecraft and transmitted to ground and to the End User with very low latency.

While the EO-ALERT concept and architecture enables a wide range of low-latency earth observation products, two use-case scenarios are developed to proof the feasibility of the approach: Ship detection and extreme weather nowcasting. The ship detection scenario is motivated by the European Maritime Safety Agency's (EMSA) vessel detection service and offers possible applications for monitorization of illegal fishing, illegal immigration, and in search and rescue missions.

In this work, the second application, meteorological nowcasting for early warnings of convective storms, is used to demonstrate the capabilities of the EO-ALERT product and its novel data processing chain in a realistic scenario. The article is organized as follows: Section 2 gives an overview of the state of convective storm nowcasting. In Section 3, the EO-ALERT processing chain is presented as a solution for low latency storm nowcasting. Sections 4 and 5 present the design and results of the detection algorithms for convective storm and Overshooting Top (OT) detection. Section 6 briefly summarizes the conclusion of this work.

2. Background

Deep moist convection processes cause damaging effects like heavy rainfall and large hail, strong wind gusts, wind shear, lightning, tornadoes, etc. Those, in turn, produce

CDCEO 2021: 1st Workshop on Complex Data Challenges in Earth Observation, virtual, Gold Coast, Australia, November 1, 2021
robert.hinz@deimos-space.com (R. Hinz); alvaro.moron@deimos-space.com (Morón); cmarcosm@aemet.es (C. Marcos)
0000-0001-7333-2477 (R. Hinz); 0000-0002-8861-7376 (C. Marcos)

negative effects like flash floods, power cuts, damaged crops, etc. which can negatively affect human lives as well as produce high economic losses [3]. Overshooting tops (OTs) are deep convective storm updrafts able to rise above the storms' equilibrium level in the tropopause region. OTs are directly related to hazardous weather at the Earth's surface such as heavy rainfall, damaging winds, large hail, and tornadoes [4]. An early detection of these kinds of phenomena is beneficial in many senses.

Meteorological forecasters use non-hydrostatic numerical prediction models (NWP) to forecast convective storm occurrence some days in advance, but the accuracy these NWP provide does not allow to know their exact location, time and intensity level. For this reason, nowcasting tasks are crucial in these cases. Nowcasting systems of the national meteorological services are mainly fed by remote sensing data like radar and satellite images, and derived products.

The international meteorological community is continuously putting a great deal of effort into the understanding of convective phenomena and the improvement of nowcasting tools. To that purpose, EUMETSAT has a dedicated Satellite Application Facility (SAF) to provide nowcasting tools (NWCSAF). In particular, the NWCSAF Rapid Developing Thunderstorms – Convection Warning (RDT-CW) product is devoted to the detection, tracking and forecasting of intense convective systems and rapidly developing convective cells [5].

The RDT-CW is a mainly satellite-based product that provides information on the storm location, size, speed, followed and future trajectory, cloud top cooling rate and severity information, among many other useful descriptive parameters. RDT-CW also performs OT detection. To compute all this information, RDT-CW uses, besides satellite imagery at different times, NWP fields, lightning information and other NWCSAF product outputs. RDT-CW has been both calibrated and validated against lightning information, and needs between three and nine minutes to be processed (depending on the region processing size and the number of NWCSAF products used as input), once raw data has been downloaded to ground, image generation has reached Level 1.5 and its radiances are available.

3. EO-ALERT Processing chain for rapid civil alerts

The low latencies required for early warnings of convective storms obtained from meteorological nowcasting and very short-range forecasting are limited by the classical EO data chain, which involves the acquisition, compression, and storage of sensor data onboard the satellite, and its transfer to ground for further processing by products like the RDT-CW. The EO-ALERT project proposes to move EO data processing elements from the ground segment to the satellite and execute image processing and machine learning algorithms onboard (O/B). Relying solely on image data acquired O/B, processing can be started as soon as a cloud cell is visible in the acquired image (Figure 1). By applying AI-based image processing, storms can thus be detected before they are seen in radar data on ground. Alerts for detected convective cells are then sent to ground on-the-fly before the actual raw data is transmitted. The alert information can trigger and complement further analysis done on ground by other existing solutions.

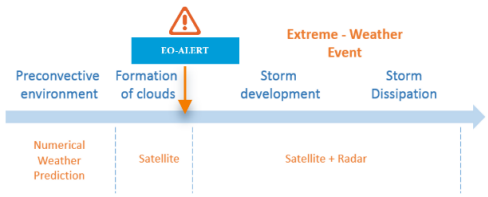

Figure 1: Data availability for forecasting and nowcasting at different stages of storm evolution.

The proposed novel satellite processing chain optimises the classical EO processing chain in a number of critical aspects and has implications on several technological areas, including high-speed avionics, Flight Segment/Ground Segment (FS/GS) communications, O/B compression and data handling and O/B image generation and processing (Figure 2). In contrast to the classical EO data processing chain this approach does not rely on the transfer of raw data to ground and thus greatly reduces the amount of data transmitted. Together with the EO-ALERT onboard data compression and high data rate communication links, this allows for very low latency product delivery. EO-ALERT has a goal latency of less than 1 min and requires a maximum latency below 5 min for both Synthetic Aperture Radar (SAR) and optical image products, including those from LEO and GEO satellites.

The Hardware (HW) design is implemented as a hybrid solution that uses both Commercial Off-The-Shelf (COTS) and space-qualified components [6, 7]. COTS are used in conjunction with mitigation techniques to increase robustness of the design against radiation effects, whereas space-qualified components are used for the critical functions. This choice allows keeping weight, volume and cost of the Payload Data Processing Unit (PDPU) low with respect to an all space-grade design and it takes advantage of the state-of-the-art technology and processing power of the latest COTS components. Processing boards are based on the Xilinx Zynq US+ ZU19EG MPSoC featuring a quad core ARM processor and a large Field-Programmable Gate Array (FPGA).

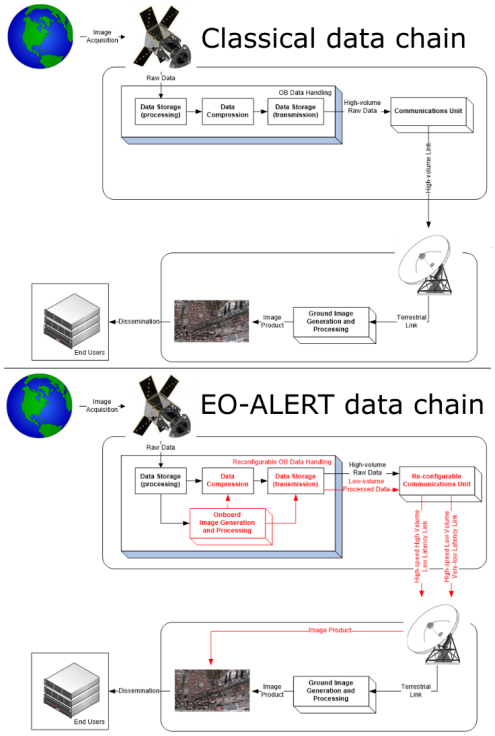

Figure 2: EO-ALERT's next generation satellite processing chain for rapid civil alerts modifies the classical data chain (black, top) based on raw data compression and transfer, by new innovative key elements and data flows (red, bottom).

The proposed processing chain is verified and evaluated for the Ship detection and Extreme Weather scenario, using relevant EO sensor data. The Extreme Weather scenario will be described in detail in the following.

4. Convective storm detection

4.1. Data

A key prerequisite for the development of AI/ML algorithms for the O/B processing chain is the availability of data sets representative of the data to be used onboard (generally uncompressed L0, L1). Optical image generation from raw data is performed by the O/B processing chain and tested for the ship scenario. The EO-ALERT dataset for the extreme weather (EW) scenario has been created from MSG High Rate SEVIRI Level 1.5 data, which is obtained from the EUMETSAT Data Centre and corresponds to 164 days in 62 periods of one or more consecutive days between 2016 and 2018. Images have size 1192pxl x 639pxl with a ground sampling distance of 3 km/px, covering a total area of 6.855.192 km² containing the European continent. Of the 12 available SEVIRI channels, 5 are used for the generation of the data set: Ch05 (WV 6.2µm), Ch06 (WV 7.3µm), Ch07 (IR Window channel 8.7µm), Ch09 (IR10.8µm), Ch10 (IR12.0µm).

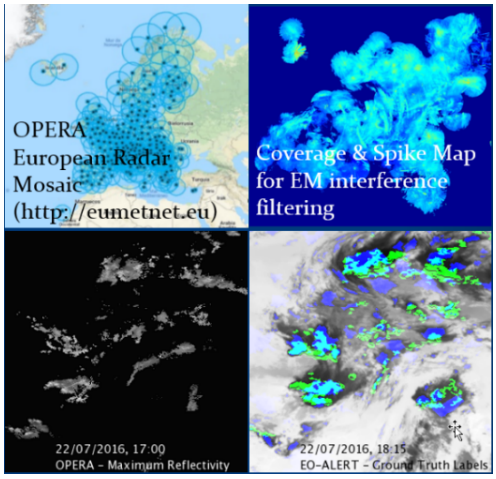

Figure 3: Ground Truth data generation from OPERA radar data.

Ground truth data for training and testing of the ML algorithm is generated from OPERA weather radar network maximum reflectivity data [8]. First, radar images corresponding to cloud-free days are used for the creation of a clutter map. Radar echoes with an intensity less than that locally defined by the clutter map are classified as spurious echoes caused by EM interferences and removed from radar images. The algorithm described in Steiner et al. [9] is then applied to detect mature convective cells in each radar image. After re-projecting OPERA images to the MSG grid, convective labels are assigned based on the spatial overlap between OPERA convective cells and EO-ALERT candidate cells detected in SEVIRI IR10.8µm images (see 4.2). Only cells within the OPERA radar network's coverage (Figure 3 top left) and a latitude below $55°0'$N are included. The ground truth Phase of Life (PoL; Convective Initiation, Mature, Decaying) is assigned to each candidate cell based on the temporal evolution of radar reflectivity, as illustrated in Figure 4: A cell which is convective in the radar image stays 'Mature' until radar reflectivity decreases below a threshold ($th_{dec} = 35dBZ$), after which it is considered 'Decaying'. Analogously, going backward in time, the PoL changes from 'Mature' to 'Convection Initiation' when passing below a fixed threshold ($th_{pre} = 35dBZ$). Cells which are not discriminated as convective in the radar image at any step of their evolution are considered non-convective, while cells at any PoL are considered convective.

The data set is split into train, validation and test set. A summary of the number of dates, images, detected

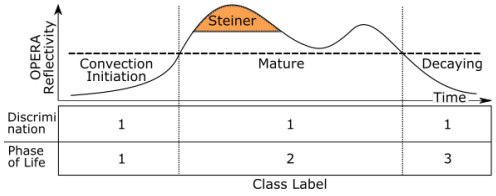

Figure 4: Classification schemes: Labels assigned for Phase of Life (CI=1, Mature=2, Decaying=3) and Convective Discrimination (Convective=1). Non-convective=0 in both cases.

Table 1
EO-ALERT EW data set information

Set	Days	Images	Cells	% Conv
Total	164	8358	2289822	26
Train	123	6369	1719448	25
Val.	17	910	275859	30
Test	24	1079	294515	27

candidate cells and the ratio of convective cells is shown in Table 1.

4.2. Image processing algorithm

Image processing and cell discrimination follows a multi-step algorithmic approach (Figure 5) inspired by the RDT-CW product. The processing steps are:

1) **Candidate Cell Extraction**: Radiances from SEVIRI IR10.8µm images are converted to brightness temperature images. Temperature minima with a temperature difference between cell top and cell base greater than $6^{\circ}C$ are detected, the cell boundaries corresponding to each minimum are found, and the candidate mask is created.

2) **Candidate Cell Tracking**: In order to gather information on the evolution and movement of cells, their trajectory is followed over subsequent acquisition times. Cells are matched to those found in the previous image based on spatial overlap in subsequent candidate maps. Ambiguities (splitting, merging of cells) as well as the disappearance and formation of cells are handled.

3) **Candidate Cell Discrimination**: Each cell is characterized by its corresponding brightness temperatures in 5 infrared channels in SEVIRI imagery and their respective evolution over time, and cell features for ML classification are created from historical information from up to 4 past and the present acquisition times ($T_H = -60, -45, -30, -15, 0$ min), combining:

- Cell area (in the candidate mask)
- Statistics on the Brightness Temperatures (BT) in 5 Channels (Minimum, Maximum, Mean)
- Intra-channel differences between different acquisition times (e.g., $\min(BT_{0min}^{IR10.8}) - \min(BT_{-15min}^{IR10.8})$)
- Inter-channel differences for same acquisition times (e.g., $\min(BT_{0min}^{IR10.8}) - \min(BT_{0min}^{WV6.2})$).

Depending on the historical information available for a cell, this results in a total number of 47, 108, 184, 275 or 381 features.

Gradient Boosting Decision Tree (GBDT) ensemble classifiers are used for discrimination of convective/non-convective cells, Phase-of-Life-classification and Overshooting Top detection. For convective discrimination and PoL, separate GBDT models were trained for each configuration of available historical information. PoL-classification is performed using a one-vs-rest scheme only on those cells which have previously been discriminated as 'convective'.

4) **Alert Generation**: Finally, alerts are created for cells which have been classified as convective. These alert messages, which contain the comprehensive characterization details of the detected storms, are transferred to ground where they can then be evaluated by the end-user.

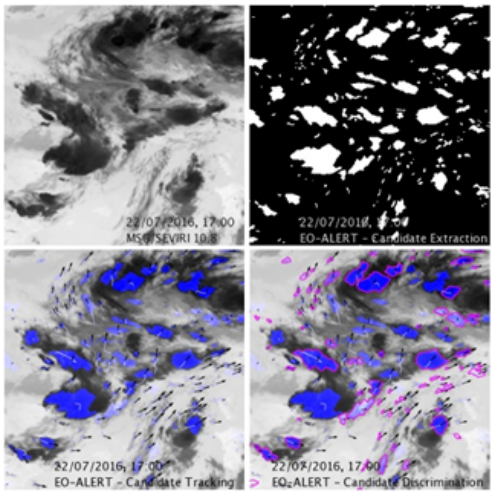

Figure 5: Extreme weather processing steps: Top left: SEVIRI IR10.8µm image. Top right: Candidate mask. Bottom left: Cell tracking. Bottom right: Cell discrimination.

4.3. Results

For performance and latency evaluation the extreme weather algorithm was executed on the EO-ALERT EW test set, setting a 366pxl x 366pxl region of interest (ROI) covering approximately $1,2$ x $10^6 km^2$ centered on the Iberian Peninsula. Results are presented for convective/non-convective discrimination.

Table 2
Extreme weather convective discrimination results on SEVIRI-OPERA test set.

History (min)	POD	FAR	F1
0, -15, -30, -45, -60	0.82	0.14	0.84
0, -15, -30, -45	0.70	0.21	0.74
0, -15, -30	0.66	0.23	0.71
0, -15	0.59	0.25	0.66
0	0.47	0.29	0.57
Combined	0.68	0.20	0.73
RDT v2018 (OPERA)	0.43	0.28	0.54
RDT v2011	0.74	0.34	-

Table 3
Elapsed processing time for optical IP on the target hardware

	Time (s)
Preprocessing	1.9s
Candidate Extraction	1.1s
Tracking	0.4s
Discrimination	0.9s
Total Elapsed Time	4.3s

Detection performance. Results in terms of Probability of Detection (POD), False Alarm Ratio (FAR) and F1-score are shown in Table 2. Performance improves (i.e., POD increases, FAR decreases) with each additional time step available, reaching POD=0.82 and FAR=0.14 for cells with fully available history. When combining the results for all history configurations (POD=0.68, FAR=0.20), performance is still compatible with the operational RDT product. The result for "RDT v2018 (OPERA)" is obtained by validating RDT convective cells versus the OPERA-derived ground truth. This is not the data RDT-CW is originally calibrated on. Due to these differences in the ground truth data and the classification strategy [5, 10, 11] the comparison should be considered as qualitative. Results shown for the RDT v2011 correspond to the official RDT validation campaign for the verification setting "Moderate Lightning Hypothesis, Statistical element trajectory" [11]. This setting is similar but not identical to the EO-ALERT "Discrimination" scheme, and values are also reported for purpose of qualitative comparison. The results suggest that for convective discrimination, the EO-ALERT EW prototype product is compatible and can compete with the RDT-CW operational product.

Latencies. Processing is performed in a dual-board scheme on only one processing board. Table 3 shows the time elapsed for candidate cell extraction, tracking and discrimination. Assuming additional transfer delays and management tasks, it is possible to have the products ready to be sent to ground in 6 seconds.

Table 4
Extreme weather Overshooting Top detection

POD	FAR	F1
0.501	0.448	0.525

5. Overshooting Top Detection

5.1. Data

The dataset used for overshooting top (OT) classification is the one described in [12]. This dataset consists of two days, 20th June 2013 and 29th July 2013. The first date contains 1365, the second 446 OTs.

The dataset has been divided into 3 sets for training, validation and testing. Training is performed over the data from the entire June 20th, validation over the data from July 29th before 16:10 and testing over the data from July 29th after 16:10.

5.2. Algorithm

Overshooting Top detection is based on the work by Kim et al. [13]. Feature extraction is performed over the IR Ch09 (10.8µm) from the candidate regions (extracted from step 3 of the convective storm detection algorithm presented in Section 4.2) where within a region of pixels a standard deviation filter and a center pixel difference filter are applied. With these two filters and a subtraction between Ch05 (6.2µm) and Ch09 (10.8µm), Ch07 (8.7µm) and Ch09 (10.8µm), and Ch10 (12.0µm) and Ch09 (10.8µm), classification is carried out using a GBDT classifier. A non-maximum suppression algorithm is applied to group close regions where the same OT has been detected.

5.3. Results

OT detection is illustrated in Figure 6. In the left picture the ground truth of [12] can be found, and in the right one, the prediction from the EO-ALERT OT detection algorithm. True positives are represented in green, false positives in red and false negatives in orange.

Figure 6: OT detection algorithm results.

Detection performance results from areas containing an OT which have been obtained over all detected candidate cells are shown in Table 4. The complete discrimi-

nation result, including convection and OT detection, is illustrated in Figure 7.

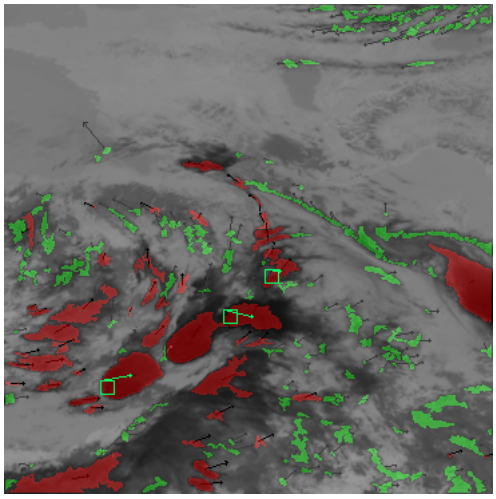

Figure 7: Illustration of final detection result. Green: Non-convective cells. Red: Convective cells. Green boxes: Overshooting Top; green lines link the OT to the center of the cell. Arrows: Direction of cell movement.

6. Conclusions

This paper provides a detailed overview of the EO-ALERT EW Scenario as a realistic application example of the EO-ALERT data processing and communication pipeline, which provides low-latency nowcasting of convective storms by performing machine learning-based EO satellite image analysis directly O/B the satellite. The modular storm detection system consisting of candidate convective cell extraction, tracking and ML-based discrimination of convective storms and overshooting tops obtains promising qualitative (comparison with the RDT-CW product) and quantitative (validation against OPERA radar data and CWG OT database) results. Results from hardware testing show that the demanding objective of providing EO products with a latency below 5 min from data acquisition to product delivery, including data handling, processing and transmission to ground, can be achieved and global EO product latencies below 1 min are feasible in realistic scenarios.

Acknowledgments

This project has been supported by the European Union and the H2020 Research and Innovation program. We thank EUMETSAT for providing MSG-SEVIRI data, EUMETNET for OPERA radar data [8], and the EUMETSAT Convection Working Group (cwg.eumetsat.int) for sharing their Overshooting Top database.

References

[1] M. Kerr, S. Cornara, A. Latorre, S. Tonetti, A. Fiengo, S. Aguero, J. I. Bravo, D. Velotto, M. Eineder, S. Jacobsen, H. Breit, O. Koudelka, F. Teschl, E. Magli, T. Bianchi, R. Freddi, M. Benetti, R. Fabrizi, S. Fraile, C. Marcos, EO-ALERT: A Novel Flight Segment Architecture for EO Satellites Providing Very Low Latency Data Products, in: Earth Observation Φ−week, 2019.

[2] S. Tonetti, S. Cornara, G. V. D. Miguel, L. Carzana, M. Kerr, R. Fabrizi, S. Fraile, C. M. Martín, D. Velotto, EO-ALERT: Next Generation Satellite Processing Chain for Security-Driven Early Warning Capacity in Maritime Surveillance and Extreme Weather Events, in: Living Planet Symposium, Milan, 2019.

[3] N. Dotzek, P. Groenemeijer, B. Feuerstein, A. M. Holzer, Overview of ESSL's severe convective storms research using the European Severe Weather Database ESWD, Atmospheric Research 93 (2009) 575–586. URL: http://dx.doi.org/10.1016/j.atmosres.2008.10.020. doi:10.1016/j.atmosres.2008.10.020.

[4] K. M. Bedka, Overshooting cloud top detections using MSG SEVIRI Infrared brightness temperatures and their relationship to severe weather over Europe, Atmospheric Research 99 (2011) 175–189. URL: http://dx.doi.org/10.1016/j.atmosres.2010.10.001. doi:10.1016/j.atmosres.2010.10.001.

[5] F. Autonès, J.-M. Moisselin, Algorithm Theoretical Basis Document for the Convection Product Processors of the NWC/GEO, 2019. URL: https://www.nwcsaf.org/web/guest/scientificdocumentation.

[6] K. LaBel, Commercial Off The Shelf (COTS): Radiation Effects Considerations and Approaches, in: NASA Electronic Parts and Packaging Program (NEPP) Electronics Technology Workshop (ETW), 2012. URL: https://nepp.nasa.gov/workshops/etw2012/talks/Tuesday/T14_LaBel_COTS_Radiation_Effects.pdf.

[7] D. Sinclair, J. Dyer, Radiation Effects and COTS Parts in SmallSats, 27th Annual AIAA/USU Conference on Small Satellites (2013) 1–12. URL: http://digitalcommons.usu.edu/smallsat/2013/all2013/69/.

[8] E. Saltikoff, G. Haase, L. Delobbe, N. Gaussiat, M. Martet, D. Idziorek, H. Leijnse, P. Novák, M. Lukach, K. Stephan, OPERA the Radar Project, Atmosphere 10 (2019) 320. doi:10.3390/atmos10060320.

[9] M. Steiner, R. A. Houze Jr., S. E. Yuter, Climatologi-

cal Characterization of Three-Dimensional Storm Structure from Operational Radar and Rain Gauge Data, Journal of Applied Meteorology 34 (1995) 1978–2007.

[10] F. Autonès, M. Claudon, Validation report of the Convection Product Processors of the NWC/GEO, 2019. URL: https://www.nwcsaf.org/web/guest/scientificdocumentation.

[11] F. Autonès, J.-M. Moisselin, Validation report of the Convection Product Processors of the NWC/GEO, 2016. URL: https://www.nwcsaf.org/web/guest/scientificdocumentation.

[12] M. Setvák, M. Radová, J. Kaňák, M. Valachová, K. M. Bedka, J. Šťástka, P. Novák, H. Kyznarová, Comparison of the MSG 2.5-minute Rapid Scan Data and Products derived from these, with Radar and Lightning Observations, EUMETSAT Proceedings (2014) 22–26.

[13] M. Kim, J. Im, H. Park, S. Park, M. I. Lee, M. H. Ahn, Detection of tropical overshooting cloud tops using himawari-8 imagery, Remote Sensing 9 (2017) 1–19. doi:10.3390/rs9070685.